 doi:10.20944/preprints201710.0128.v1

Article

Lignin-Depolymerisation via UV-Photolysis and Titanium Dioxide Photocatalysis

Xuan Tung Do[1], Basma El Khaldi-Hansen[1], Anke Nietsch[2], Christian Jung[2], Steffen Witzleben[1] and Margit Schulze[1]*

[1] Department of Natural Sciences, Bonn-Rhein-Sieg University of Applied Sciences, Von-Liebig-Straße 20, 53359 Rheinbach, Germany; xuan-tung.do@h-brs.de
[2] Institute of Solar Research and Solar Chemical Engineering, German Aerospace Centre, Linder Höhe, 51147 Köln, Germany; christian.jung@dlr.de
* Correspondence: margit.schulze@h-brs.de; Tel.: +49-2241-865-566; Fax: +49-2241-865-8566

Abstract: Today, more than 70 million tons of lignin are produced by the pulp and paper industry every year. However, the utilization of lignin as a source for chemical synthesis is still limited due to the complex and heterogeneous lignin structure. The purpose of this study was a selective photodegradation of industrially available kraft lignin in order to obtain appropriate fragments and building block chemicals for further utilization, e.g. polymerization. Thus, kraft lignin obtained from soft wood black liquor by acidification was dissolved in sodium hydroxide and irradiated at a wavelength of 254 nm with and without the presence of titanium dioxide in various concentrations. Analyses of the irradiated products via SEC showed decreasing molar masses and decreasing polydispersity indices over time. At the end of the irradiation period the lignin was depolymerised to form fragments as small as the lignin monomers. TOC analyses showed minimal mineralisation due to the depolymerisation process.

Keywords: kraft lignin; photolysis; photocatalysis; actinometry; OH-number; SEC; UV-VIS; ATR-FTIR; XRD

1. Introduction

Currently 95 % of all chemical substances are produced from petroleum. In view of the limited occurrence and the rapid exhaustion of fossil resources, the efforts of many scientists are focusing on the use of alternative sources [1]. One of the most promising alternatives could be lignin, which is the third most common biopolymer on earth. Lignin is a complex, three-dimensional irregularly cross-linked polymer which, as a constituent of woody plants, makes up one third of the dry mass of the wood in addition to cellulose and hemicellulose [2]. Being produced as a by-product in the pulp and paper industry in an amount of about 70 million tons per year, it is currently used solely as a renewable combustible raw material for energy generation [3]. Despite recovery, some of the lignin still finds its way into the environment with the wastewater. Since lignin is very resistant to microbial degradation, it cannot completely be removed by conventional wastewater treatment techniques [4].

An approach to overcome this difficulty is to irradiate the effluents with ultraviolet light (UV) in the presence of titanium dioxide (TiO_2) as a catalyst. By indirect photolysis and heterogeneous photocatalysis, organic impurities such as lignin can completely be mineralised to carbon dioxide and water [5]. However, the mechanism for wastewater treatment can also be used for controlled depolymerisation of lignin. As it is a natural aromatic macromolecule, organic chemicals and valuable substances can be extracted. Current work by Hansen *et al.* investigating the degradation process on solid organosolv lignin using pyrolysis GC/MS showed pure lignin fractions and phenolic products originating from monolignols [6]. Alvarado-Morales *et al.* performed TiO_2/UV-based photocatalytic degradation and quantified vanillic acid and ferulic acid as main organic products. They found different yields of these products by varying reaction parameters such

 doi:10.20944/preprints201710.0128.v1

as irradiation time and catalyst concentration [7]. Nair *et al.* studied the photocatalytic lignin fragmentation to enhance the contact between lignin and TiO_2 and thus improved the degradation process. The phenolic products were identified via GC/MS [8]. Xu and colleagues recently summarized recent advances in the selective decomposition of lignin-based compounds via photocatalysis in a critical review [9].

This scientific work includes the photolytic and photocatalytic degradation of lignin at the molecular level. Influences of irradiation time and photocatalyst concentration on the degradation process were investigated. The degradation products were analysed by chromatography (SEC), spectroscopy (ATR-FTIR, UV-VIS) and wet-chemistry (OH-number, total organic carbon (TOC)).

2. Results

2.1. X-Ray Powder Diffraction of the Photocatalyst

The photocatalyst used for the experiments was analysed using X-ray powder diffraction. Using the software Bruker Diffrac.EVA, the crystallinity was determined. The provided AEROXIDE P25® shows a crystalline and amorphous share of 90.5 % and 9.5 %, respectively. As titanium dioxide naturally exists in three different crystal modifications, namely anatase, rutile and brookite [9], and these have different photocatalytic activities, the three modifications were quantified using Rietveld refinement (Bruker Diffrac.TOPAS). The provided titanium dioxide is found to be 85.49 % anatase, 14.30 % rutile and 0.21 % brookite. Considering the amorphous share, the total composition is 77.4:12.9:0.2:9.5 (anatase:rutile:brookite:amorphous share).

2.2. Characterisation of the Annular Reactor

As the radiation output of the used UV-lamp is not constant over its entire life span, the performance of the lamp was evaluated before and after the experimental program using Hatchard/Parker-actinometry. The UV-radiation output was 15’800 mW at the beginning and 12’200 mW at the end. To estimate the actual output at the beginning of each irradiation experiment, the determined outputs were interpolated in a linear fashion.

2.3. Total Hydroxyl Group Determination

For future synthesis of polyurethanes, the knowledge of the total hydroxyl group content is important. Therefore, this parameter was determined using a method based on ISO 14900:2001 (E). Figure 1 shows the development of the hydroxyl group content over the course of the irradiation experiment. As the withdrawn sample volume of 300 mL each compared to the starting volume of 5’000 mL is not insignificant and the radiation output remains almost constant during the experiment, the radiation power needs to be weighted for the volume which is irradiated. With proceeding irradiation times, a decrease in total hydroxyl group content can be observed, independent from the catalyst concentration being used.

Preprints (www.preprints.org) | NOT PEER-REVIEWED | Posted: 18 October 2017 doi:10.20944/preprints201710.0128.v1

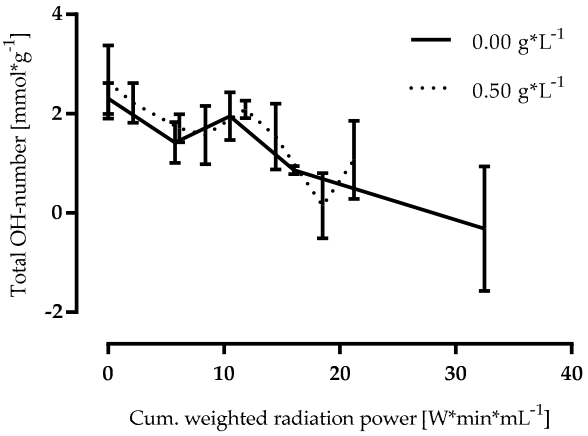

Figure 1. Total hydroxyl group content of the irradiated lignins plotted versus the cumulated weighted radiation power.

2.4. pH-Value

The pH-value of the lignin solutions was monitored during the irradiation process and is depicted in Figure 2. A decrease in pH-value can be observed for all experiments, independent from the catalyst concentration being used.

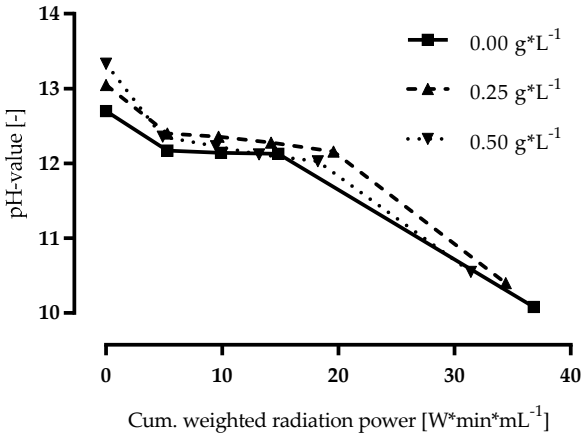

Figure 2. pH-values of the lignin solutions during the irradiation process.

2.5. Total Organic Carbon

As depicted in Figure 3 the content of total organic carbon (TOC) decreases with the proceeding irradiation process while the content of inorganic carbon (IC) increases. A correlation between the catalyst concentration and decrease of TOC or increase of IC cannot be observed.

Preprints (www.preprints.org) | NOT PEER-REVIEWED | Posted: 18 October 2017 doi:10.20944/preprints201710.0128.v1

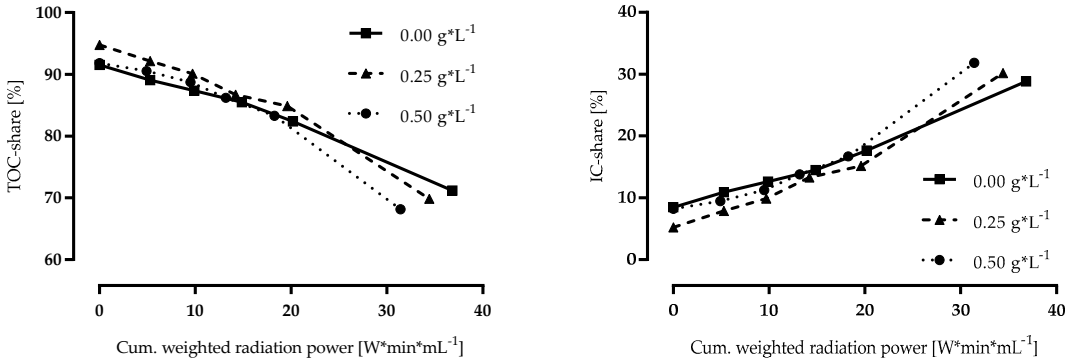

Figure 3. (a) TOC and (b) IC of the lignin solutions during the irradiation process.

2.6. Size Exclusion Chromatography

To evaluate the impact of the irradiation process on the molecular weight of lignin, size exclusion chromatography was performed on the isolated samples. Figure 4a shows the molar weight distribution of the lignins isolated from the irradiation experiment using 0.25 g*L^{-1} of the catalyst. All curves are normalised so that changes in the shape of the curves can be evaluated more easily. The longer the lignin solution was irradiated, the more the maximum of the respective curve is shifted towards smaller molar weights. Furthermore, the width of the respective curve decreases with the proceeding irradiation process. Figure 4b shows the changes in the number average molar weight for all the irradiation experiments. All curves show the same trend. The number average molar weight decreases over the course of the irradiation experiment, independent from the catalyst concentration being used.

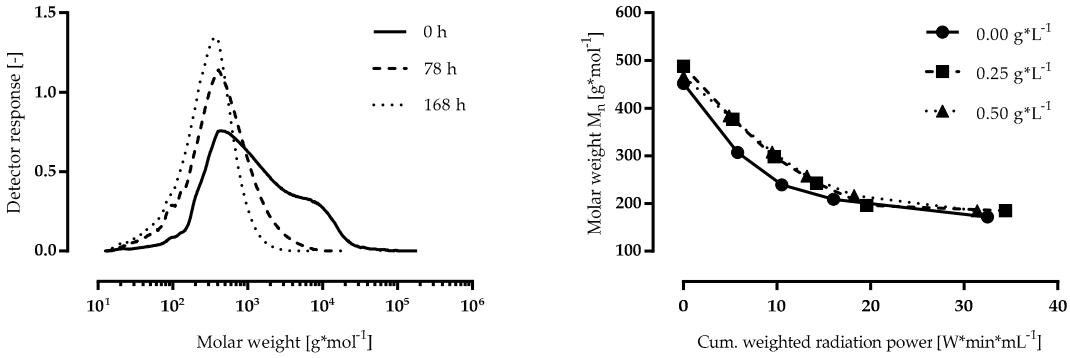

Figure 4. (a) Molar weight distribution of the lignins isolated. The areas under the curves are normalised. (b) Changes in number average molar weight (Mn).

2.7. UV-VIS Spectroscopy

UV-VIS-spectra of the irradiated and isolated lignins were recorded in aqueous sodium hydroxide. As all spectra look similar, the spectra of the lignins from the irradiation experiment using 0.00 g*L^{-1} of the catalyst are depicted in Figure 5. For easier comparison, the spectra are normalised to their maximum. The unirradiated lignin shows an absorption shoulder at 280-295 nm, which gradually disappears with the proceeding irradiation process until it cannot be identified anymore.

Preprints (www.preprints.org) | NOT PEER-REVIEWED | Posted: 18 October 2017 doi:10.20944/preprints201710.0128.v1

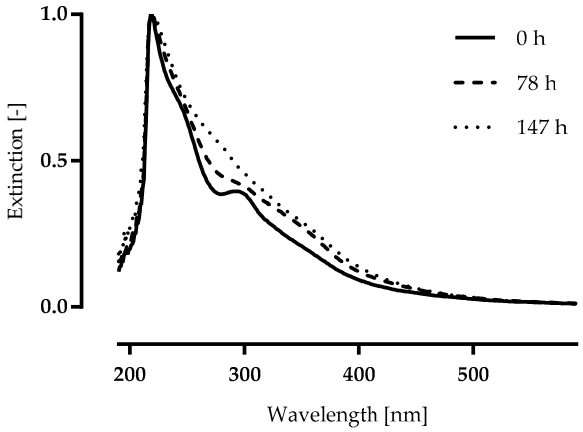

Figure 5. UV-VIS-spectra of the irradiated lignins. Spectra are height normalised.

2.8. ATR-FTIR Spectroscopy

FTIR-spectra of the lignins were recorded using the ATR technique. Since the spectra of the different irradiation experiments almost look the same, only the spectra of the experiment using 0.25 g*L^{-1} are depicted in Figure 6.

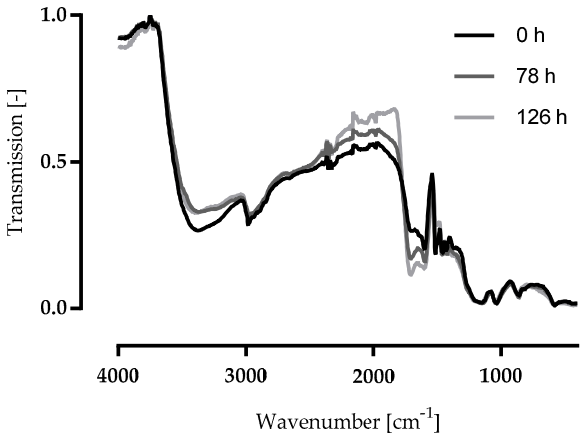

Figure 6. ATR-FTIR-spectra of the irradiated lignins.

An assignment of the absorption bands to the functional groups is shown in Table 1. Comparing the FTIR-spectra shows that the absorption band at 3'380 cm^{-1} which is caused by the hydroxyl group in relation to the band at 2'980 cm^{-1} decreases with the irradiation progress. Relating the band at 1'700 cm^{-1} to the band at 1'600 cm^{-1} an increase of the band at 1'700 cm^{-1} can be observed. A decrease of the bands at 1'510 cm^{-1} and 1'460 cm^{-1} can also be observed.

Preprints (www.preprints.org) | NOT PEER-REVIEWED | Posted: 18 October 2017 doi:10.20944/preprints201710.0128.v1

Table 1. Assignment of the absorption bands to the functional groups.

Measured wavenumber [cm^{-1}]	Typical wavenumber [cm^{-1}]	Vibrational mode
3'380	3'650-3'200	O-H stretching vibration
2'980	3'000-2'840	C-H stretching vibration in -CH, -CH_2 or -CH_3
1'700	1'707-1'690	C=O stretching vibration (conjugated)
1'600	1'625-1'575	arC-C vibration
1'510	1'525-1'475	arC-C vibration
1'460	1'475-1'430	Asymmetric deformation vibration of -CH_2 and -CH_3

3. Discussion

Analysis of the degraded lignins showed that the total hydroxyl group content decreases with increasing irradiation times. This observation was also made by Wang *et al.* who discovered a reduction of phenolic hydroxyl group content by up to 41 % [11]. The herein presented results suggest a reduction of total hydroxyl group content by up to 100 %.

These results must be interpreted with caution, as all samples were prepared by acidic precipitation without further washing. As acidity of the samples was not corrected for, remaining acid from the precipitation process might interfere with the results. However, the same trend could be validated by means of ATR-FTIR.

The recorded ATR-FTIR-spectra indicate a reduction of OH-stretching vibration (3'380 cm^{-1}) in relation to the aliphatic CH-stretching vibration (2'980 cm^{-1}) and simultaneously an increase of the conjugated C=O-stretching vibration (1'700 cm^{-1}). At the same time, a decrease of aromatic vibrations (1'510 cm^{-1} and 1'460 cm^{-1}) can be observed. As the TiO_2/UV-process is described to have an oxidative mechanism it is plausible that hydroxyl groups are first oxidised to form carbonic acids and then ultimately mineralised to carbon dioxide and water [12]. Wang *et al.* postulated a mechanism for the formation of carbonic acids from lignin depicted in Figure 7.

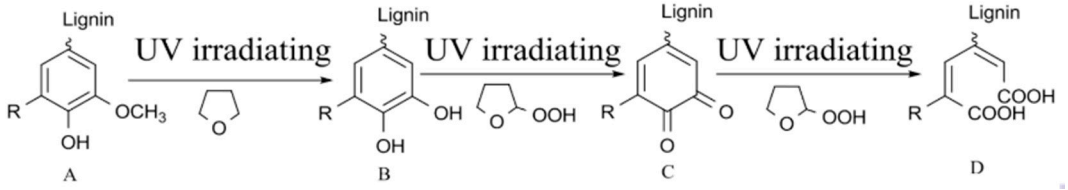

Figure 7. Reaction mechanism for the decolourisation of lignin via UV-irradiation in THF. Reproduced from Wang *et al.* [11].

The formation of carbonic acids and carbon dioxide might also be a possible explanation for the decrease in pH-value. Figure 7 shows the destruction of the aromatic ring which is consistent with the findings obtained by ATR-FTIR as well as UV-VIS spectroscopy.

UV-VIS spectroscopy shows an absorption shoulder for untreated lignin at 280-295 nm which can be assigned to the structure of the monomers coniferyl alcohol and sinapyl alcohol [13]. The dissolution of this absorption shoulder correlates with the decrease of aromatic vibrations and strengthens the evidence for the destruction of the aromatic ring suggested by Wang *et al.* [11].

The formation of carbon dioxide was proven by TOC measurements indicating an increase of inorganic carbon content. This observation can be explained by partial mineralization of lignin (30 %), further proving the oxidative character of the TiO_2/UV process. Carbon dioxide formation could also be observed by Ohnishi *et al.* by means of gas chromatography [12].

As it was intended to depolymerise lignin, size exclusion chromatography is the method of choice for evaluating the lignin fragments. Prado *et al.* investigated the depolymerisation of organosolv lignin showing a reduction in molar weight from 941 g*mol^{-1} down to 763 g*mol^{-1} [14].

 doi:10.20944/preprints201710.0128.v1

As a matter of fact, our results even show a decrease from approx. 500 g*mol^{-1} down to 170 g*mol^{-1} correlating with the average molar weight of the lignin monomers of 180 g*mol^{-1} (paracoumaryl alcohol: 150 g*mol^{-1}, coniferyl alcohol: 180 g*mol^{-1}, sinapyl alcohol: 210 g*mol^{-1}).

Since the commercial catalyst AEROXIDE P25® is a mixture of titanium dioxide modifications with anatase being the photocatalytically most active one, the composition was determined using x-ray powder diffraction together with Rietveld refinement. The total composition of the provided AEROXIDE P25® was 77.4:12.9:0.2:9.5 (anatase:rutile:brookite:amorphous share) confirming the findings of Ohtani *et al.* reporting a composition of 78:14:8 (anatase:rutile:amorphous share) [15].

Although the provided photocatalyst could positively be identified as the highly active AEROXIDE P25®, no significant differences regarding the analytical results could be observed, when comparing the catalyst concentrations used. One plausible explanation could be that on the one hand the used catalyst:lignin ratio was too low and on the other hand the lignin concentration was too high. Previous studies reported catalyst:lignin ratios of 50:1 [11], 5:1-200:1 [16] or 1:1,8-1,6:1 [17]. The catalyst:lignin ratios used by us (0:1-1:10) and the high lignin concentration might result in total absorption of UV-radiation solely by lignin, thus leading to a pure photolysis instead of photocatalysis, rendering the photocatalyst ineffective as described by Kansal *et al.* [16]. A reduction of chemical oxygen demand and UV-absorption was also observed by Chang *et al.* who investigated the degradation of lignin via pure photolysis [5].

4. Materials and Methods

4.1. Precipitation of Lignin from Black Liquor

Kraft-lignin was isolated from soft wood black liquor by acidic precipitation. Prior to acidification, the black liquor provided by ZPR (Rosenthal, Germany) was vacuum filtrated using filter papers with 12-15 µm particle retention. Under constant stirring sulfuric acid (25 vol. %) was added dropwise. After reaching a pH-value of 2 the suspension was stirred for another 1 h before it was centrifuged at 3'000 rpm for 15 mins. For washing, the supernatant was discarded, replaced with deionised water, re-suspended and centrifuged again. The washed lignin (3 times) was then freeze-dried for 48 h.

4.2. Irradiation Experiments

For the irradiation process a reactor comprising a water-cooled quartz annulus with an UV-lamp (UVX 60 by UV-Technik, Germany), a 5 L reservoir and a centrifugal pump was used. The previously prepared lignin was dissolved in aqueous sodium hydroxide solution (5 g*L^{-1} in 0.1 mol*L^{-1}) and added with different amounts of AEROXIDE P25® (0.00 g*L^{-1}, 0.25 g*L^{-1} and 0.50 g*L^{-1}). 5 L of the solution were irradiated at room temperature for up to 7 days and samples of 300 mL were taken daily.

4.3. Isolation of Fragmented Lignins

For further analysis, the irradiated lignins were isolated in a process analogue to the process mentioned above. Instead of precipitating the irradiated lignins at a pH-value of 2, which usually gives the highest yield [18], a pH-value of 1 was chosen, as some of the irradiated lignins remain dissolved at a pH-value of 2. Also, the precipitated lignins were not washed, as some of the lignins even were soluble in deionized water. Prior to acidification the AERODIDE P25® was removed by vacuum filtration using filter papers with 0.45 µm particle retention.

4.4. Hatchard/Parker Actinometry

The characterisation of the annular reactor was performed as described by Hatchard and Parker 1953. Before the actinometry could be performed, the apparatus including all sample containing glassware were completely covered in aluminium foil, as the reaction used to determine the UV-power is sensitive to light. For the quantification of Fe^{2+}-ions in form of the ferroin-complex a calibration in a range of 0.04-8.00 mg*L^{-1} was prepared. In addition, 5 L of a 50 mmol*L^{-1}

 doi:10.20944/preprints201710.0128.v1

potassium-ferrioxalate solution was prepared. After a pre-heating phase of the UV-lamp 12 samples of 3 mL were taken within 12 mins and incubated with phenanthroline for 1 h. The samples were then analysed using a UV-VIS-spectrometer at 510 nm (Lambda 19 by Perkin Elmer, USA).

4.5. OH-Number Determination via Acetylation

For the determination of the OH-number a procedure based on ISO 14900:2001 (E) was used. Modifications were made regarding the acetylation temperature and time as well as the sample amount and the amount of the acetylation reagent. Thus, 25 mg of the lignins were weighed into a 1.5 mL reaction vessel and added with 850 µL acetylation reagent. Inspired by Clauss *et al.* [19] and Baumberger *et al.* [20], who acetylated their samples at room temperature for 20 h and 6 days, respectively, an acetylation time of 72 h at room temperature was chosen. Excess of acetic anhydride was titrated with 0.2 mol*L^{-1} sodium hydroxide using an automated titrator (Stabino PMX 400 by Particle Metrix, Germany). All measurements were repeated 6 times.

4.6. Total Organic Carbon (TOC)

For TOC analysis, all samples taken from the reactor were diluted 1/20 in 0.1 mol*L^{-1} aqueous sodium hydroxide and measured in triplicates (TOC-L by Shimadzu, Japan).

4.7. Size-exclusion Chromatography (SEC)

To evaluate the depolymerisation of the lignins SEC was performed using the parameters shown in Table 2. Samples with a concentration of 2 mg*mL^{-1} were prepared in THF and filtrated with 0.2 µm PTFE filters prior to analysis. For molar weight evaluation polystyrene was used as a calibration standard.

Table 2. SEC set up and parameters.

Component	Description	Parameter
Eluent	THF p.a.	HPLC-grade
Pump	Agilent 1100 Series	Flowrate: 1.000 mL*min^{-1}
Injector	Rheodyne 7725i sample loop	Injection volume: 100 µL
Oven	Agilent 1100 Series	Temperature: 35 °C
Column	1x PSS SDV 8*50 mm pre-column	Particle size: 5 µm
	2x PSS SDV 8*300 mm Linear M 5µ	Particle size: 5 µm Molar weight range: 50-10'000'000 g*mol^{-1}
Detector	Agilent 1100 Series VWD	Wavelength: 280 nm
Calibration	PSS ReadyCal-Kit Polystyren	Calibration range: 376-2'570'000 g*mol^{-1}

4.8. UV-VIS Spectroscopy (UV-VIS)

UV-VIS-spectra were recorded in a wavelength range of 190-800 nm (DR 6000 by Hach Lange, Germany) using 10 mm quartz cuvettes. Therefore 5 mg of the lignins were dissolved in 100 mL of 0.1 mol*L^{-1} aqueous sodium hydroxide [21].

4.9. ATR-FTIR Spectroscopy (ATR-FTIR)

ATR-FTIR-spectra were recorded in a wavenumber range of 4'000-400 cm^{-1} with a resolution of 4 cm^{-1} (Vertex 70 and Platinum ATR Diamond by Bruker, USA). For noise reduction, each sample was measured 96 times. Since the irradiated lignins were not washed after precipitation all spectra had to be compensated for the presence of sodium hydrogen sulphate.

 doi:10.20944/preprints201710.0128.v1

4.10. Powder X-ray Diffraction (XRD)

The characterisation of AEROXIDE P25® was performed using a bench top x-ray diffractometer (D2 PHASER by Bruker, USA) with the parameters described in Table 3.

Table 3. XRD set up and parameters.

Parameter	Settings
Detector	Lynxeye, 5.86002946944° opening angle
Tube	Cu-anode, 1.54184 □, 30 kV, 10 mA
Scan type, mode	Coupled two theta/theta, continuous PSD fast
Rotation	0 rpm
2 Theta	10.002026596-65.002026596°, Δ=0.010173662275°
Theta	5.001013298-32.501013298°, Δ=0.005086831138°
Steps	5’407
Time per step	0.500 s

5. Conclusions

This study aimed to describe the impact of UV irradiation time and catalyst concentration on the photocatalytical or rather the photolytical depolymeration of lignin into valuable chemical building blocks. Using a variety of analytical methods (chromatography, spectroscopy and wet-chemistry) it could be shown that the lignin was selectively depolymerised to the size of its monomers and even partially mineralised proving the oxidative character of the degradation process. For the chosen catalyst concentration no significant differences could be found confirming the photolytical origin of the lignin fragmentation process.

Acknowledgments: Financial support by Federal Ministry of Education and Reserach (BMBF) program “Forschung an Fachhochschulen“ project FKZ03FH013IX4.

Author Contributions: Xuan Tung Do: main part including lignin isolation and photolysis studies, result development, wrote the paper; Basma El Khaldi-Hansen: support in writing; Anke Nietsch: support in photocatalytic experiments, in particular long-term studies; Christian Jung: conducting the experimental setup for photolysis and photocatalysis; Steffen Witzleben: planning studies, lignin isolation and XRD studies; Margit Schulze: planning studies, conducting experimental investigation and results discussion, coordination of writing and editing.

Conflicts of Interest: The authors declare no conflict of interest.

References

1 Beller, M., Centi, G., Sun, L., Chemistry Future: Priorities and Opportunities from the Sustainability Perspective. *Chem Sus Chem* **2017**, *10*, pp. 6–13.

2 Chen, L. et al., Conversion of lignin model compounds under mild conditions in pseudo-homogeneous systems. *Green Chem* **2016**, *18*, pp. 2341-2352.

3 Fang, Z.; Smith, R.L., Jr. Production of Biofuels and Chemicals from Lignin; Springer Science + Business Media Singapore: Singapore, **2016**; Chapter 1; pp. 3–33.

4 Ma, Y.S. et al., Photocatalytic degradation of lignin using Pt/TiO2 as the catalyst. *Chemosphere* **2008**, *71*, pp. 998-1004.

5 Chang, C.N. et al., Decolorizing of lignin wastewater using the photochemical UV/TiO2 process. *Chemosphere* ***2004***, *56*, pp. 1011-1017.

6 Hansen, B. et al., Qualitative and quantitative analysis of lignin produced from beech wood by different conditions of the organosolv process. *J Polym Environ* **2016**, *24*, pp. 85-97.

7 Alvarado-Morales, M. et al., TiO2/UV based photocatalytic pretreatment of wheat straw for biogas production. *Anaerobe* **2016**, *in press*.

8 Nair, V. et al., Production of phenolics via photocatalysis of ball milled lignin-TiO2 mixtures in aqueous suspension. *RSC Adv*. **2016**, *6*, pp. 18204-18216.

9 Shao-Hai Li, Siqi Liu, Juan Carlos Colmenares and Yi-Jun Xu, A sustainable approach for lignin valorization by heterogeneous photocatalysis. Green Chem., 2016, 18, 594–607.

10 Akpan, U.G., Hameed, B.H., Parameters affecting the photocatalytic degradation of dyes using TiO2-based photocatalyst: A review. *J Hazard Mater* **2009**, *170*, pp. 520-529.

11 Wang, H. et al., ZnCl2 induced catalytic conversion of softwood lignin to aromatics and hydrocarbons. *Green Chem* **2016**, *18*, pp. 2802-2810.

12 Ohnishi, H. et al., Bleaching of lignin solution by a photocatalyzed reaction on semiconductor photocatalyst. *Ind Eng Chem Res* **1989**, *28*, pp. 719-724.

13 Jablonsky,M. et al., Characterization and comparison by UV spectroscopy of precipitated lignins and commercial lignosulfonates. *Cell Chem Technol* **2015**, *3-4*, pp. 267-274.

14 Prado, R. et al., Effect of the photocatalytic activity of TiO2 on lignin depolymerisation. *Chemosphere* **2013**, *91*, pp. 1355-1361.

15 Ohtani, B. et al., What is Degussa (Evonic) P25? Crystalline composition analysis, reconstruction from isolated pure particles and photocatalytic activity test. *J Photoch Photobio A* **2010**, *216*, pp. 179-182.

16 Kansal, S.K. et al., Studies on TiO2/ZnO photocatalysed degradation of lignin. *J Hazard Mater* **2008**, *153*, pp. 412-417.

17 Kumar, P. et al., Titanium dioxide photocatalysis for the pulp and paper industry water treatment. *Indian J Sci Technol* **2011**, *4*, pp. 327-332.

18 Toledano, A. et al., 2009. Characterization of lignins obtained by selective precipitation, *Seperation and Purification Technology*, 68. Jg., pp.193-198.

19 Clauss, M.M. et al., 2015. Size-Exclusion Chromatography and Aggregation Studies of Acetylated Lignins in N,N-Dimethylacetamide in the Presence of Salts. *Macromolecular Chemistry and Physics*, 216(20), pp.2012–2019.

20 Baumberger, S. et al., 2007. Molar mass determination of lignins by size-exclusion chromatography: Towards standardisation of the method. *Holzforschung*, 61(4), pp.459–468.

21 Gonzalez Arzola, K. et al., 2006. Early attack and subsequent changes produced in an industrial lignin by a fungal laccase and a laccase-mediator system: an analytical approach. *Applied Microbiology and Biotechnology*, 73, pp.141-150.